Low-temperature phase transition in nanostructured MnO embedded within the channels of MCM-41-type matrices

I. V. Golosovsky,[1] I. Mirebeau,[2] F. Fauth,[3] D. A. Kurdyukov,[4] and Yu. A. Kumzerov[4]
[1]*St. Petersburg Nuclear Physics Institute, 188300, Gatchina, St. Petersburg, Russia*
[2]*Laboratoire Léon Brillouin, CE-Saclay, F-91191, Gif-sur-Yvette, France*
[3]*ESRF, Polygone Scientifique Louis Néel, 6 rue Jules Horowitz, 38000 Grenoble, France*
[4]*A. F. Ioffe Physico-Technical Institute, 194021 St. Petersburg, Russia*
(Received 7 April 2006; revised manuscript received 5 June 2006; published 29 August 2006)

High-resolution x-ray-diffraction experiments of antiferromagnetic MnO nanostructured within the channels of mesoporous MCM-41 matrices reveal an unusual transition from a distorted, trigonal phase to a cubic phase at about 40 K, well below the magnetic transition temperature of 120 K. The disappearance of the structural distortion is accompanied by an increase of the unit-cell parameter, amplitude of atomic motion, and the appearance of inner stresses. Such behavior drastically differs from the behavior known for the bulk compound.

DOI: 10.1103/PhysRevB.74.054433 PACS number(s): 75.75.+a, 61.46.-w, 61.10.Nz, 64.70.Nd

Since the discovery in 1949 of antiferromagnet ordering in manganese oxide (MnO),[1] this compound has been a subject of much experimental and theoretical interest.

In this oxide, the antiferromagnetic ordering, which appears around 117 K, is accompanied by a rhombohedral contraction of the cubic lattice along the [111] axis.[2,3] Magnetic structure consists of ferromagnetic sheets stacked antiferromagnetically along the [111] axis.[4,5] In such a structure, known as type II in the face-centered-cubic lattice,[6] magnetic moments in the first coordination sphere are frustrated.

Greenwald and Smart in the early 1950s suggested that the structural distortion, which is concomitant with the magnetic ordering, removes the frustration and minimizes the exchange energy.[7] So an elastic anisotropic deformation and magnetic order are mutually dependent.

The effects of exchange-induced distortion of a cubic lattice were first considered in the mean-field approximation.[3] It was shown that the difference in the exchange integrals between the nearest parallel spins and the nearest antiparallel spins due to the structural distortion stabilizes the magnetic structure. Later, by the random-phase Green's function method, Lines and Jones demonstrated that this difference provides a discontinuous first-order magnetic transition.[8]

During the past decade, studies of confined nanomagnets became a very active field of research. The reason is fundamental since the confined geometry and the influence of the surface yields unusual physical properties as compared with the bulk.

Nanostructured MnO appeared to be a very attractive compound for such investigations. First, in this antiferromagnet, magnetic and nuclear reflections are well separated. Secondly, MnO can be synthesized within porous media in a quantity, which allows the diffraction studies.

Our systematic investigation of MnO in confinement started with MnO embedded in a Vycor-type glass matrix with a random network of pores[9] and continued with MnO within MCM-41-type matrices with a regular system of nanochannels. These silica matrices known as mesoporous molecular sieves [or Mobil Company Material (MCM)] were discovered in 1992.[10] The performed studies revealed remarkable differences in the properties of confined MnO with the bulk.

MnO confined within a porous glass forms on the average isotropic aggregates, while MnO confined to the channels of MCM matrices crystallizes in the form of thin (about 10 Å) ribbonlike structures or nanowires.[11] In all cases, the nanoparticle lengths are in the interval of 180–260 Å increasing with the channel diameter. From high-resolution x-ray diffraction and electron spin resonance (ESR) experiments,[12] we found that in addition to crystalline MnO, a large amount of amorphous MnO is present within the channels.

Neutron-diffraction experiments demonstrated that the magnetic structure observed in nanostructured MnO was the same as in the bulk.[9,13] The volume-averaged magnetic moment of confined MnO calculated from the magnetic reflection intensity turns out to be noticeably smaller than the bulk value that can be readily explained by the disorder of the moments at the surface.

The discontinuous magnetic transition in the bulk becomes a continuous transition with an enhanced Néel temperature with respect to the bulk. For the channel-type matrices, the character of the magnetic transition transforms with decreasing channel diameter. The critical exponent and Néel temperature decrease, which was attributed to the increasing anisotropy of the magnetic system.[13]

Because of the low resolution of the neutron powder diffraction experiments, it is not possible to measure the structure distortions in confined MnO with sufficient precision. So to study the structural distortions, we used the high-resolution x-ray diffraction. The present work addresses the results of these experiments.

EXPERIMENTAL DETAILS

The experiments were performed with MnO embedded within the matrices MCM-41 with 24 and 35 Å channel diameters (referred to below as MCM) and SBA-15 matrices with 47, 68, and 87 Å diameters (referred to below as SBA). All matrices were prepared in the Laboratoire de Chimie Physique, Université Paris-Sud, France.[14] MnO was synthe-

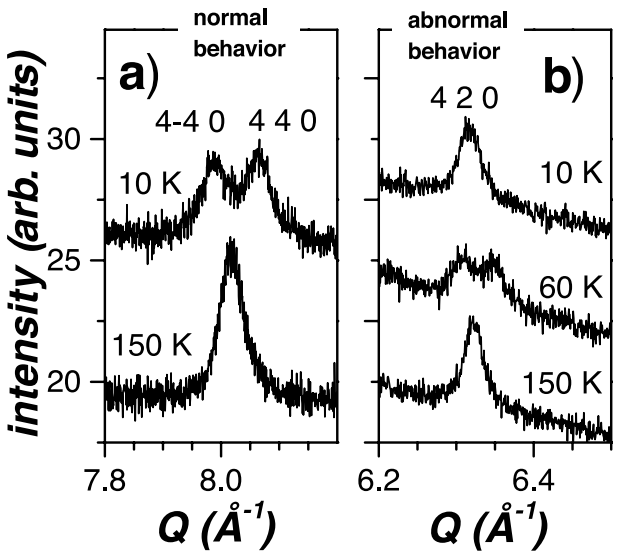

FIG. 1. (a) Normal behavior of the x-ray-diffraction patterns of MnO within MCM with 87 Å the channel diameter above (150 K) and below (10 K) the magnetic transition; (b) abnormal behavior of the patterns of MnO within MCM with 35 Å channel diameter.

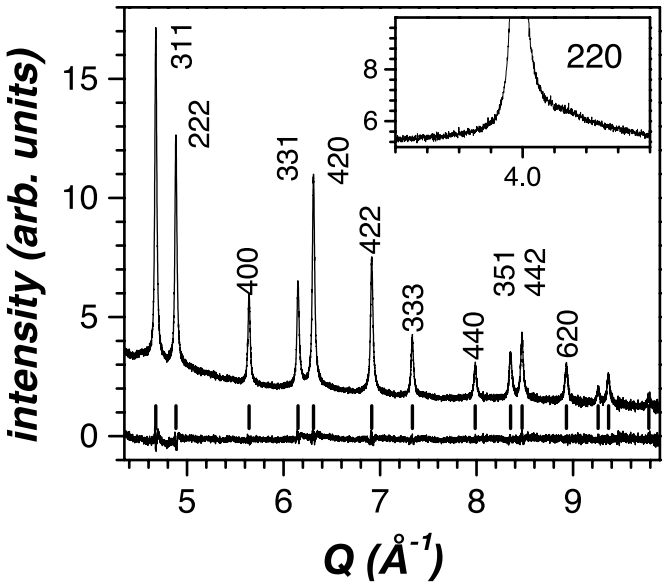

FIG. 2. The x-ray-diffraction patterns of MnO within MCM with 35 Å channel diameter at 10 K. In the bottom, the difference of calculated and observed profiles is shown. Bars mark the reflection position. In the inset the enlarged fragment of the pattern is shown.

sized within the nanochannels by the "bath deposition" method.

Matrices MCM and SBA differ in the technology of preparation, and all represent an amorphous silica (SiO_2) body pierced by the parallel channels. The channels form a regular honeycomb system in a section with the averaged wall thickness between the adjacent channels of about 10 Å slightly (about 1–2 Å) different for different matrices.

We used two sets of the samples referred to below as "old" and "new," which differs by the quantity of the embedded MnO in the same matrices. The full sample characterization had been given in Refs. 11–13. The consistent analysis of neutron diffraction, x-ray diffraction, and ESR ensures that MnO predominantly occupies the channel voids.

X-ray-diffraction experiments were performed at the beamline ID31 of the European Synchrotron Radiation Facility with wavelengths of 0.800 and 0.500 Å. To avoid preferred orientation effects, the powder samples sealed in 1 mm quartz capillaries were rotated continuously during the experiment. An Oxford Instruments continuous flow cryostat was used.

RESULTS AND DISCUSSION

As expected, below the magnetic transition, the diffraction reflections split due to the trigonal distortion. As an example, in Fig. 1(a), a fragment of x-ray pattern measured for SBA with 87 Å channel diameter is shown above (150 K) and below (10 K) the magnetic transition.

Unexpectedly, for two samples (MCM with 35 Å channel diameter and SBA with 68 Å channel diameter) we observe that the structural distortion disappears below about 40 K [Fig. 1(b)]. The crystal structure of MnO becomes cubic at low temperatures and it is above the magnetic transition.

From our previous experiments with MnO within channel-type matrices[11–13] it was known that this oxide gradually transforms (at a typical time scale of several months) to an amorphous state without any intermediate crystal phases. To check the reproducibility of the phenomenon, we prepared two new samples using the same MCM matrices with 35 and 24 Å channel diameters, for which abnormal and normal behavior had been observed, respectively. The repeated experiments were conducted with x-ray wavelength 0.5 Å instead of 0.8 Å before.

Because of improved technology, we succeeded in filling the matrix with a greater quantity of crystalline MnO. From a comparison of the ratio of the Bragg reflections to the diffuse background, it follows that the new samples with the same host matrices, i.e., the same contribution to a diffraction pattern, have a higher ratio of crystalline to amorphous MnO within the channels.

It turns out that the diffraction line shape from the new samples has a so called "saw-tooth" profile indicative of a ribbonlike form of the embedded nanoparticles[11] (inset in Fig. 2). Note that in the old sample with a smaller quantity of crystalline MnO, the diffraction peaks are symmetrical, which corresponds to a wirelike form of nanoparticles.

The complicated line shape limits the profile analysis to high angles where the "sawtooth" profile is not strongly expressed. The fragment of a profile refinement of the x-ray pattern for the new sample of MCM with 35 Å channel diameter is shown in Fig. 2. We did not detect any nonstoichiometry for all studied samples.

In Fig. 3(a), the temperature dependences of the angle of trigonal distortion and the unit-cell parameter are shown for old and new MCM with 35 Å channel diameter. For comparison, the dependence for the sample with normal behavior, namely SBA with 87 Å channel diameter, is shown too.

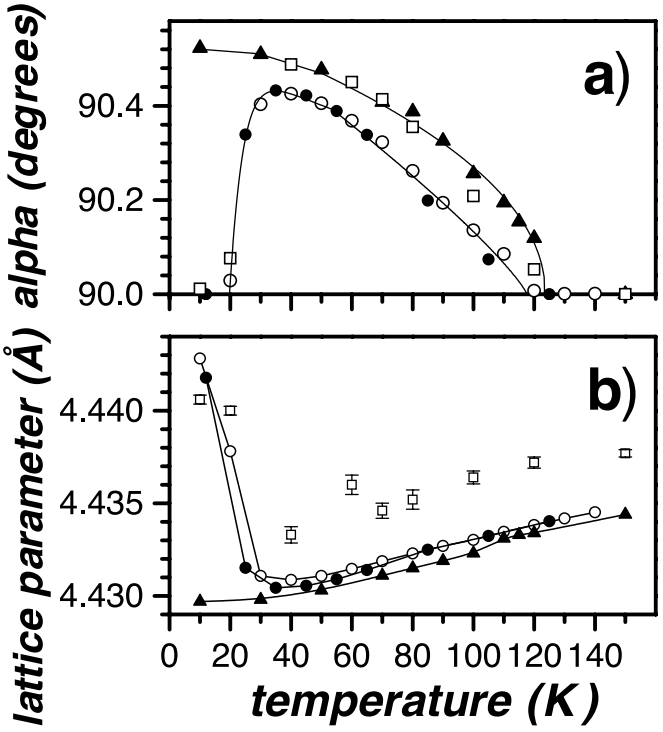

FIG. 3. Temperature dependences of the angle of trigonal distortion (alpha) (a) and the lattice parameter (b). Open circles corresponds to new MCM with 35 Å channel diameter at warming, closed circles at cooling; open squares corresponds to old MCM at warming; solid triangles correspond to SBA with 87 Å channel diameter (normal behavior). Errors (e.s.d., estimated standard deviation), if not shown, do not exceed the symbol size.

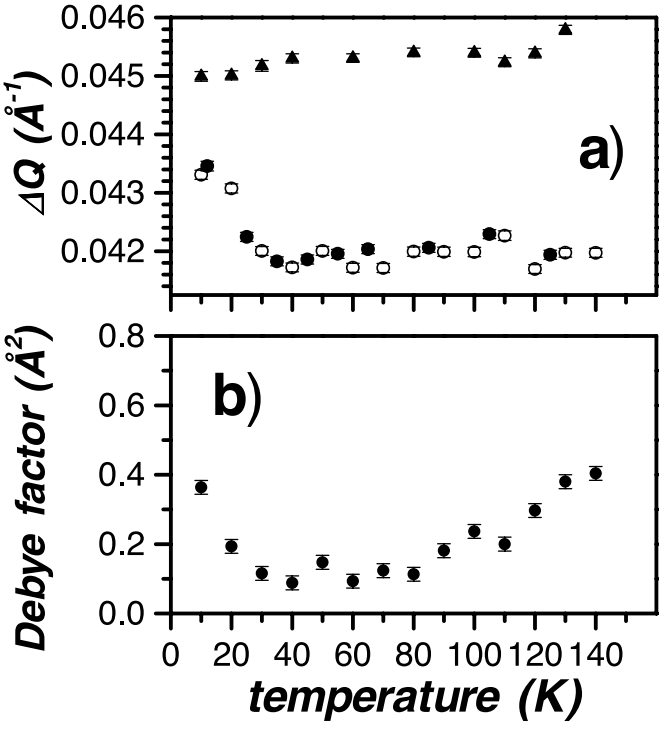

FIG. 4. (a) Temperature dependences of the FWHM for reflection 200 for MCM with 35 Å channel diameter with abnormal behavior. Open circles, warming; closed circles, cooling; solid triangles correspond to MCM with 24 Å channel diameter and normal behavior. (b) Temperature dependence of the Debye parameter for MCM with 35 Å channel diameter. Errors (e.s.d.), if not shown, do not exceed the symbol size.

The "reentrant" effect is observed at cooling as well as at warming.

Both MCM samples with 35 Å channel diameter, new and old, show an abnormal behavior, namely a sharp decrease of the distortion angle below 40 K. Both samples MCM with 24 Å channel diameters, old and new, show a normal behavior, namely a continuous increase of the distortion angle down to the lowest temperature.

In Fig. 3(b) it is seen that the disappearing structural distortions in the samples with abnormal behavior are accompanied by a sharp increase of the lattice parameter.

The difference in the absolute values of the lattice constants for two samples, old and new, is readily explained by the different form of the embedded nanoparticles: ribbonlike and wirelike. It is well known that in the case of a two-dimensional lattice (ribbonlike form), the maxima of diffraction peaks do not coincide with the nodes in the reciprocal space, which leads to an underestimation of the unit-cell parameter.[11,15] Note that in SBA with 87 Å channel diameter and normal behavior, the nanoparticles have a ribbonlike form.

Together with the sharp change of structure parameters, we discovered a change in the full width at half maximum (FWHM) of the diffraction peaks, which takes place together with the disappearance of the structural distortion. In Fig. 4(a), the FWHM (in the reciprocal space) is shown for the reflection 200, which does not split at the trigonal distortion.

Because the instrumental linewidth is different by some percent from the measured peak width, the observed FWHM coincides with the peak broadening ΔQ. Therefore, the difference in FWHM for MCM's with 35 and 24 Å channel diameters [Fig. 4(a)] is readily explained by the difference in the nanoparticle shape. The nanoparticles within the thinner channels are smaller so the corresponding FWHM is larger.

It had been pointed out[16] that the magnetic structure in MnO with spins perpendicular to the triad axis is inconsistent with rhombohedral symmetry, so the true symmetry should be lower. However, a special search carried out for the bulk[17] did not show any deviation from the rhombohedral symmetry below the magnetic transition. In experiments with nanostructured MnO, we did not detect any deviations from the rhombohedral symmetry nor from the cubic symmetry at low temperatures as well.

So we assume that the observed peak broadening, ΔQ, originates from size effect or inner stresses only. In the first case $\Delta Q(Q)$ does not depend on the reciprocal-lattice vector Q, while in the second case it should be proportional to Q. In Fig. 5, the dependences $\Delta Q(Q)$ for some temperatures are shown. They are shown for high Q only, since the effects of the "sawtooth" profile at low Q are too strong.

The experimental peak broadening has a temperature and Q-independent contribution, which is attributed to the size effect, and a linear contribution whose slope is proportional to the inner stresses. In Fig. 5 it is seen that additional

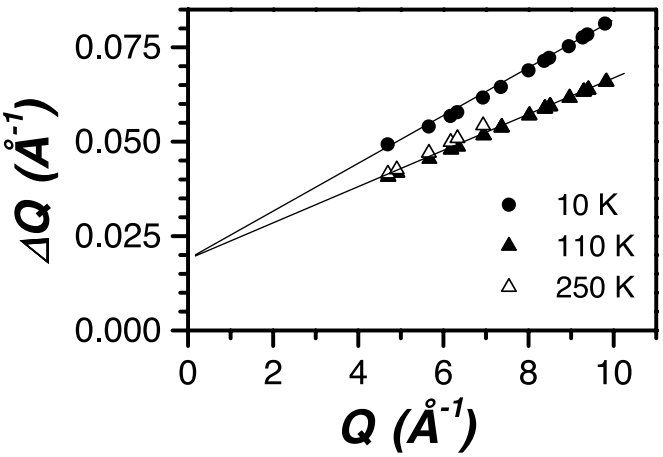

FIG. 5. Q dependences of the peak broadening for MCM with 35 Å channel diameter and abnormal behavior for temperatures 250, 140, and 10 K. Errors (e.s.d.) do not exceed the symbol size.

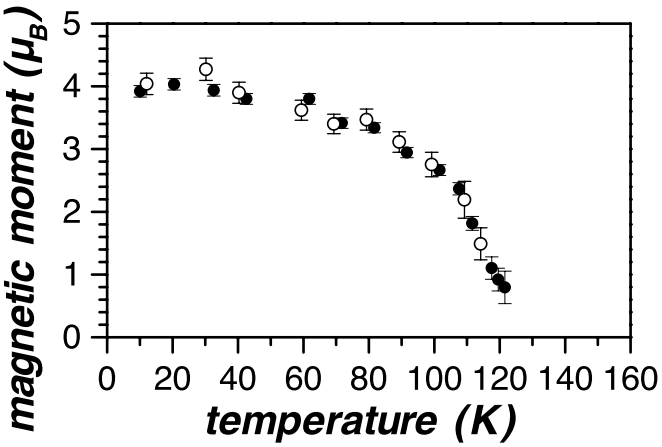

FIG. 6. Temperature dependence of the magnetic moment in MCM with 35 Å channel diameter calculated from the intensity of the magnetic reflection $\frac{1}{2}\frac{1}{2}\frac{1}{2}$. Closed and open circles belong to two sets of data measured in an interval of about two years.

stresses should be associated with the low-temperature transition.

The disappearance of the structural distortions is accompanied with an increase of the Debye-Waller parameter, which is proportional to the mean-square displacement of atoms [Fig. 4(b)].

The observation of sharp changes in the structure parameters and the appearance of the inner stresses strongly evidences that we are dealing with a specific low-temperature phase transition, a new original phenomenon observed in confinement only and unknown before.

It was mentioned above that the low-temperature transition was observed in SBA with the channel diameter of 67 Å as well. It is worthwhile to note that the channel diameter and the transverse dimensions of the ribbonlike or wirelike nanoparticles are not in direct relation. We can claim only that the transverse dimensions cannot be larger than the channel diameter.

In conventional theory, the antiferromagnetic state in MnO is stabilized by the structural distortions. The theory predicts the angle of trigonal distortion to be proportional to the square of the magnetic moment.[3,8] However, in the case of nanoparticles, the high anisotropy and the inner stresses add new terms in the free energy, which could drastically change the energy balance.

In our neutron-diffraction measurements, we observed the antiferromagnetic order in all studied samples.[13] As an example, the temperature dependences of the magnetic moment for MCM with abnormal behavior are shown in Fig. 6. Surprisingly, there is no change in the temperature dependence of the ordered magnetic moment accompanied with the low-temperature transition.

Today we do not know the real mechanism that triggers the discovered phase transition. Investigations of this surprising phenomenon should be continued by other methods, in particular by the measurements of antiferromagnetic resonance, susceptibility, and others.

In conclusion, high-resolution x-ray-diffraction experiments performed with nanoparticles of antiferromagnetic MnO confined to the channels of MCM-41-type matrices showed the existence of a new low-temperature structural transition, which is accompanied by the disappearance of the structural distortion, an increase in the unit-cell parameter and in the amplitude of atomic motion, and the appearance of the inner stresses. Such behavior drastically differs from the behavior known for the bulk compound.

ACKNOWLEDGMENTS

The authors are grateful to S. B. Vakhrushev and S. L. Ginsburg for a critical reading of the manuscript and fruitful discussions. The work was supported by Grants No. RFBR-04-02-16550, No. SS-1671-2003.2, No. INTAS-2001-0826, and the program RAN "Effect of Atomic Crystalline and Electronic Structure on the Properties of Condensed Matter."

[1] C. G. Shull and J. S. Smart, Phys. Rev. **76**, 1256 (1949).
[2] C. P. Bean and D. S. Rodbell, Phys. Rev. **126**, 104 (1962).
[3] D. S. Rodbell and J. Owen, J. Appl. Phys. **35**, 1002 (1964).
[4] C. G. Shull, W. A. Strauser, and E. O. Wollan, Phys. Rev. **83**, 333 (1951).
[5] W. L. Roth, Phys. Rev. **110**, 1333 (1958).
[6] J. S. Smart, *Effective Field Theories of Magnetism* (W. B. Saunders Company, Philadelphia, 1966).
[7] S. Greenwald and J. S. Smart, Nature (London) **165** 523 (1950); Phys. Rev. **82**, 113 (1951).
[8] M. E. Lines and E. D. Jones, Phys. Rev. **141**, 525 (1966).
[9] I. V. Golosovsky, I. Mirebeau, G. André, D. A. Kurdyukov, Yu. A. Kumzerov, and S. B. Vakhrushev, Phys. Rev. Lett. **86**, 5783 (2001).

[10] C. T. Kresge, M. E. Leonowicz, W. J. Roth, J. C. Vartuli, and J. S. Beck, Nature (London) **359**, 710 (1992).
[11] I. V. Golosovsky, I. Mirebeau, E. Elkaim, D. A. Kurdyukov, and Y. A. Kumzerov, Eur. Phys. J. B **47**, 55 (2005).
[12] I. V. Golosovsky, D. Arčon, Z. Jagličič, P. Cevc, V. P. Sakhnenko, D. A. Kurdyukov, and Y. A. Kumzerov, Phys. Rev. B **72**, 144410 (2005).
[13] I. V. Golosovsky, I. Mirebeau, V. P. Sakhnenko, D. A. Kurdyukov, and Y. A. Kumzerov, Phys. Rev. B **72**, 144409 (2005).
[14] D. Morineau, G. Dossen, and C. Alba-Simionesco, Philos. Mag. B **79**, 1845 (1999).
[15] B. E. Warren, Phys. Rev. **59**, 693 (1941).
[16] A. K. Cheetham and D. A. Hope, Phys. Rev. B **27**, 6964 (1983).
[17] W. Jauch, and M. Reehuis, Phys. Rev. B **67**, 184420 (2003).